

# On the accuracy of modified Stokes's integration in high-frequency gravimetric geoid determination

P. Novák<sup>1</sup>, P. Vaniček<sup>1</sup>, M. Véronneau<sup>2</sup>, S. Holmes<sup>3</sup>, W. Featherstone<sup>3</sup>

<sup>1</sup> Department of Geodesy and Geomatics Engineering, University of New Brunswick, Fredericton, Canada E3B 5A3  
e-mail: pnovak@ucalgary.ca; Tel.: +1 403 617 9157; Fax: +1 403 284 1980

<sup>2</sup> Geodetic Survey Division, Natural Resources Canada, 615 Booth Street, Ottawa, Canada K1A 0E9

<sup>3</sup> School of Spatial Sciences, Curtin University of Technology, GPO BOX U1987, Perth WA 6845, Australia

Received: 2 November 1999 / Accepted: 11 July 2000

**Abstract.** Two numerical techniques are used in recent regional high-frequency geoid computations in Canada: discrete numerical integration and fast Fourier transform. These two techniques have been tested for their numerical accuracy using a synthetic gravity field. The synthetic field was generated by artificially extending the EGM96 spherical harmonic coefficients to degree 2160, which is commensurate with the regular 5' geographical grid used in Canada. This field was used to generate self-consistent sets of synthetic gravity anomalies and synthetic geoid heights with different degree variance spectra, which were used as control on the numerical geoid computation techniques. Both the discrete integration and the fast Fourier transform were applied within a 6° spherical cap centered at each computation point. The effect of the gravity data outside the spherical cap was computed using the spheroidal Molodenskij approach. Comparisons of these geoid solutions with the synthetic geoid heights over western Canada indicate that the high-frequency geoid can be computed with an accuracy of approximately 1 cm using the modified Stokes technique, with discrete numerical integration giving a slightly, though not significantly, better result than fast Fourier transform.

**Key words:** Geoid determination – Stokes's integration – Fast Fourier transform

## 1 Introduction

The gravimetric determination of the geoid relies upon the solution of the spherical geodetic boundary-value

problem, and requires the evaluation of Stokes's surface convolutive integral. In practice, the gravimetric geoid is computed using a combination of terrestrial and satellite-derived gravity data. The approach taken in this contribution is to spectrally decompose the geoid height into the reference spheroid (low-frequency geoid), which is computed from a satellite-derived spherical harmonic global model, and the high-frequency geoid, which is computed from terrestrial gravity data.

The high-frequency component of the geoid in this data combination requires the numerical evaluation of the adapted Stokes's formula (Stokes 1849). Generally, its solution can be obtained by:

- (1) using discrete numerical integration (i.e. quadrature-based summation)
- or
- (2) converting Stokes's convolutive integral from the space domain into a product of the spectra of Stokes's function (or a modification thereof) with that of gravity data in the frequency domain, and back again.

The latter method is usually referred to as the fast Fourier transform (FFT) technique (see e.g. Schwarz et al. 1990). Since only the one-dimensional FFT (1D-FFT; Haagmans et al. 1993) allows for evaluation of Stokes's formula without any planar approximation or simplification of the kernel, it is considered here to be the only realistic alternative to discrete numerical integration.

The major purpose of this contribution is to examine the numerical accuracy of both approaches based on the use of the Molodenskij-modified spheroidal Stokes's formula (Vaniček and Kleusberg 1987; see also Vaniček and Sjöberg 1991; Martinec and Vaniček 1996). The integration domain for the modified Stokes integral is divided into a spherical cap of radius 6° about each computation point, and the remainder of the sphere. The contribution of the gravity data within the spherical cap is computed using both discrete numerical integration and the 1D-FFT technique. The contribution of the distant gravity data in the region outside this spherical

*Correspondence to:* P. Novák  
Department of Geomatics Engineering,  
The University of Calgary,  
2500 University Drive N.W., Calgary, Canada T2N 1N4

cap is computed by employing the spectral Molodenskij-type approach (Vaníček and Sjöberg 1991).

A synthetic gravity field based on spherical harmonics will be used to assess and compare the accuracy of the gravimetrically computed geoid models (cf. Tziavos 1996). The coefficients to degree 360 of the EGM96 spherical harmonic model of the Earth's gravity field (Lemoine et al. 1998) were supplemented with synthetically generated high-frequency coefficients out to degree 2160. The EGM96 and synthetically generated coefficients were used to create self-consistent gravity anomalies and geoid heights on a regular 5' geographical grid over a test area in the Canadian Rocky Mountains. These synthetic gravity data grids were used to compute the high-frequency geoid via discrete numerical integration and the 1D-FFT technique. The difference between the computed and synthetic geoid heights was used to assess the relative numerical accuracy of these methods and the high-frequency geoid determination based on the Molodenskij-modified spheroidal Stokes formula.

## 2 Spectral decomposition of the geoid

Terrestrial gravity data provide detailed local information about the medium- and high-frequency components of the Earth's gravity field. However, due to incomplete gravity data coverage (and availability) and long-wavelength biases in the observed gravity data (e.g. due to the drift of gravimeters), the long-wavelength components of the Earth's gravity field are less accurately determined by terrestrial gravity observations. At present, the only reliable global information about the Earth's gravity field is based on artificial-satellite dynamics (i.e. the analysis of satellites' orbital perturbations). However, due to the attenuation of the strength of the Earth's gravity field with increasing distance from the geocentre, only the low-frequency component of the Earth's gravity field can reliably be detected in this way.

In the following, a spectral form of the Earth's gravity field is used, with a distinction made between the low- and high-frequency components. The threshold value of  $l = 20$  is used throughout the text. This reflects our belief that the frequencies up to this degree can correctly be derived from satellite dynamics, and do not have to be further improved by terrestrial gravity data in a combined global geopotential model. However, this choice of  $l = 20$  is somewhat subjective and no proof is given to justify this value, apart from the arguments in the preceding paragraph.

Based on the above frequency decomposition of gravity data, the geoid height can similarly be decomposed into the low-frequency *reference spheroid*  $N_l$ , and the so-called *residual geoid*  $N^l$ , which is the high-frequency component of the geoid. The reference spheroid is computed from the low-frequency gravity disturbing potential  $T_l$  at the geoid level  $r_g$  (estimated from the low-degree spherical harmonic coefficients of a global geopotential model) as follows (Bruns 1878; Heiskanen and Moritz 1967):

$$N_l(\Omega) = \frac{T_l(r_g, \Omega)}{\gamma} = \frac{GM}{r_g \gamma} \sum_{n=2}^l \left(\frac{R}{r_g}\right)^n T_n(\Omega) \doteq R \sum_{n=2}^l T_n(\Omega) \quad (1)$$

where  $\gamma$  is the normal gravity acceleration on the surface of the geocentric reference ellipsoid,  $GM$  is the product of the Newtonian gravitational constant  $G$  and the mass of the Earth  $M$ ,  $T_n$  are the zonal coefficients of the disturbing gravity potential  $T$  (derived from fully-normalized, unitless spherical harmonic coefficients obtained from a global geopotential model), and  $R$  is the radius of the geocentric reference sphere upon which the spherical harmonic expansion of the coefficients  $T_n$  reduces to the Laplace harmonics. Throughout the following, spherical coordinates  $(r, \varphi, \lambda) = (r, \Omega)$ , represented by the geocentric latitude  $\varphi$ , the geocentric longitude  $\lambda$ , and the length of the geocentric radius vector  $r$ , are used to describe a location of points of interest. The expression on the right-hand side of Eq. (1) is derived for the spherical approximation of the geoid by the reference sphere, i.e.  $r_g \doteq R$ , and for  $GM/R^2 \doteq \gamma$ .

## 3 Review of the spheroidal Molodenskij approach

This section provides a review of the spheroidal Molodenskij approach to high-frequency geoid computation as developed and used at the University of New Brunswick. The theoretical bases for these approaches are given elsewhere in the geodetic literature (see e.g. Vaníček and Kleusberg 1987; Vaníček and Sjöberg 1991; Martinec and Vaníček 1996). This section simply presents them in a single, coherent framework, which describes how to implement them practically for high-frequency geoid computation.

The geodetic boundary-value problem is used for the solution of the high-frequency gravimetric geoid that is residual to the reference spheroid. It is assumed that there are no external topographical and atmospheric masses above the geoid (i.e. the regularization of the geoid is not described or considered in this contribution). Accordingly, the high-frequency disturbing gravity potential  $T^l$  is a harmonic function everywhere outside the geoid and its behaviour is controlled by the Laplace differential equation (see e.g. Heiskanen and Moritz 1967)

$$\forall r > r_g : \nabla^2 T^l(r, \Omega) = 0 \quad (2)$$

The boundary condition to the homogeneous elliptical equation [Eq. (2)] for the solution of the unknown function  $T^l$  at the geoid level  $r_g$  is the fundamental gravimetric equation, which reads in a spherical approximation as (Martinec and Vaníček 1996)

$$r = r_g : -\Delta g^l(\Omega) \doteq \frac{\partial}{\partial r} T^l(r, \Omega) \Big|_r + \frac{2}{R} T^l(r, \Omega) \quad (3)$$

where the high-frequency gravity anomaly at the geoid is defined as (see e.g. Heiskanen and Moritz 1967)

$$\begin{aligned}\Delta g^l(\Omega) &= \Delta g(\Omega) - \frac{GM}{r_g^2} \sum_{n=2}^l \left(\frac{R}{r_g}\right)^n (n-1) T_n(\Omega) \\ &\doteq \Delta g(\Omega) - \gamma \sum_{n=2}^l (n-1) T_n(\Omega)\end{aligned}\quad (4)$$

The solution of Eqs. (2) and (3) for the unknown function  $T^l$  exists and is unique when  $T^l$  is regular at infinity and when  $\Delta g^l$  do not contain any first-degree harmonics (see e.g. Heiskanen and Moritz 1967), which can be satisfied by the proper selection of the geocentric reference ellipsoid. The solution is given by the spheroidal Stokes integral (Martinec and Vaníček 1996; see also Vaníček and Kleusberg 1987; Vaníček and Sjöberg 1991), which is analogous to the spherical Stokes (1849) integral

$$T^l(r_g, \Omega) = \frac{R}{4\pi} \iint_{\Omega_{\oplus}} \Delta g^l(\Omega') \mathcal{S}^l(\psi) d\Omega' \quad (5)$$

where  $\Omega$  defines the geocentric position of the computation point on the geoid,  $\Omega'$  defines the geocentric position of the integration point,  $\Omega_{\oplus}$  denotes the surface of a sphere of unit radius, and  $\psi$  is the spherical distance between the integration point and computation point.

The function  $\mathcal{S}^l$  for the computation of the high-frequency geoid in Eq. (5) is the spheroidal Stokes kernel (Vaníček and Kleusberg 1987), and can conveniently be computed according to

$$\mathcal{S}^l(\psi) = \mathcal{S}(\psi) - \sum_{n=2}^l \frac{2n+1}{n-1} P_n(\cos \psi) \quad (6)$$

where  $\mathcal{S}$  is the spherical Stokes kernel (Stokes 1849). The high-frequency geoid  $N^l$  can be computed from the high-frequency disturbing potential  $T^l$  using Bruns's theorem (Bruns 1878)

$$N^l(\Omega) = \frac{T^l(r_g, \Omega)}{\gamma} \quad (7)$$

which is then added to the reference spheroid  $N_l$  in Eq. (1) to yield the total geoidal height  $N$ .

Due to the incomplete coverage or availability of terrestrial gravity data, the spheroidal Stokes integral [Eq. (5)] cannot be evaluated over the full spatial angle  $\Omega_{\oplus}$ . Therefore, a limited integration domain  $\Omega_{\odot}$ , represented by a spherical cap of radius  $\psi_{\odot}$ , must be used instead (Fig. 1). This term is called the contribution of the near zone  $N_{\odot}^l$ , which can be computed from the terrestrial gravity data using the modified spheroidal Stokes integral

$$N_{\odot}^l(\Omega) = \frac{R}{4\pi\gamma} \iint_{\Omega_{\odot}} \Delta g^l(\Omega') \mathcal{S}^l(\psi, \psi_{\odot}) d\Omega' \quad (8)$$

The solution of the convolutive integral in Eq. (8) can be computed in either the spatial or the spectral form. While the former method uses discrete numerical integration of high-frequency gravity data, the latter method converts the integral from the space domain into the product of spectra of the Stokes function with that

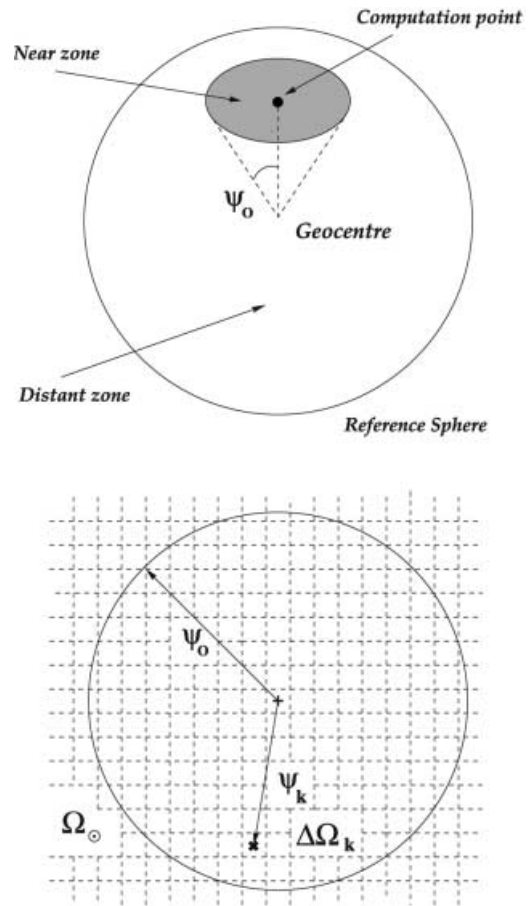


Fig. 1. Integration sub-domains in Stokes's integration

of the high-frequency gravity data in the frequency domain, and back again; see Sect. 3.2. The accuracy of these two approaches will be investigated later in this paper. Problems arising from the singularity of Stokes's integral for  $\psi = 0$  are addressed in Sect. 3.1.

The influence of the gravity information from the remainder of the globe ( $\Omega_{\oplus} - \Omega_{\odot}$ ) is accounted for using a term called the contribution of the far zone  $N_{\oplus-\odot}^l$  (the truncation bias)

$$N_{\oplus-\odot}^l(\Omega) = \frac{R}{4\pi\gamma} \iint_{\Omega_{\oplus-\odot}} \Delta g^l(\Omega') \mathcal{S}^l(\psi, \psi_{\odot}) d\Omega' \quad (9)$$

The contribution of the far zone can be evaluated from the global geopotential model, see Sect. 3.3. However, due to significant differences between available models (see e.g. Najafi 1996; also see Lambeck and Coleman 1983), one should try to keep the far zone contribution as small as possible. This can be achieved by modifying the spheroidal Stokes function. It is acknowledged that there are many different modifications to Stokes's formula. However, these will not be considered here since the modification introduced by Vaníček and Kleusberg (1987) is used for practical geoid computations in Canada.

The modified spheroidal Stokes function can be written as (Vaníček and Kleusberg 1987)

$$\forall t_n \in \mathcal{R}^n : \mathcal{S}^l(\psi, \psi_o) = \mathcal{S}^l(\psi) - \sum_{n=2}^l \frac{2n+1}{n-1} P_n(\cos \psi) - \sum_{n=0}^l \frac{2n+1}{2} t_n(\psi_o) P_n(\cos \psi) \quad (10)$$

where  $t_n$  are the modification coefficients. It can be shown that in order to minimize the effect of gravity from the remote zones, [see Eq. (9)], the following integral must be minimized (Vaníček and Kleusberg 1987):

$$\forall t_n \in \mathcal{R}^n : \min_{t_n} \left\{ \int_{\psi=\psi_o}^{\pi} [\mathcal{S}^l(\psi, \psi_o)]^2 d\Omega' \right\} \quad (11)$$

The solution leads to the system of linear equations for the unknown modification coefficients  $t_n$

$$m \leq n : \sum_{n=0}^l \frac{2n+1}{2} R_{n,m}(\psi_o) t_n(\psi_o) = Q_m^l(\psi_o) \quad (12)$$

where the coefficients  $R_{n,m}(\psi_o)$ , introduced by Paul (1973), are

$$m \leq n : R_{n,m}(\psi_o) = \int_{\psi=\psi_o}^{\pi} P_n(\cos \psi) P_m(\cos \psi) \sin \psi d\psi \quad (13)$$

The spheroidal truncation coefficients in Eq. (12) can then be computed as (cf. Molodenskij et al. 1960; see also Heiskanen and Moritz 1967; Martinec 1993)

$$Q_m^l(\psi_o) = \int_{\psi=\psi_o}^{\pi} \mathcal{S}^l(\psi) P_m(\cos \psi) \sin \psi d\psi = Q_m(\psi_o) - \sum_{n=2}^l \frac{2n+1}{n-1} R_{n,m}(\psi_o) \quad (14)$$

### 3.1 Contribution of the computation point

The spherical, spheroidal and modified spheroidal Stokes integrals are weakly singular for the spherical distance  $\psi = 0$ . Therefore, in seeking the solution in the spatial form, an appropriate treatment must first be chosen. The classical method consists of adding and subtracting the gravity anomaly at the computation point, as follows:

$$N_{\odot}^l(\Omega) = \frac{R}{4\pi\gamma} \iint_{\Omega_o} \{ \Delta g^l(\Omega) \mathcal{S}^l(\psi, \psi_o) + [\Delta g^l(\Omega') - \Delta g^l(\Omega)] \mathcal{S}^l(\psi, \psi_o) \} d\Omega' \quad (15)$$

which can be split into the contribution of the computation point

$$N_{\diamond}^l(\Omega) = \frac{R\Delta g^l(\Omega)}{2\gamma} \int_{\psi=0}^{\psi_o} \mathcal{S}^l(\psi, \psi_o) \sin \psi d\psi \quad (16)$$

and the contribution of the rest of the cap

$$N_{\odot-\diamond}^l(\Omega) = \frac{R}{4\pi\gamma} \iint_{\Omega_o} [\Delta g^l(\Omega') - \Delta g^l(\Omega)] \mathcal{S}^l(\psi, \psi_o) d\Omega' \quad (17)$$

The singularity is removed from Eq. (17) because the value of the integrand equals zero for  $\psi = 0$ . The integral of the Stokes function in Eq. (16) can be evaluated analytically as follows:

$$\begin{aligned} \int_{\psi=0}^{\psi_o} \mathcal{S}^l(\psi, \psi_o) \sin \psi d\psi &= \int_{\psi=0}^{\psi_o} \mathcal{S}^l(\psi) \sin \psi d\psi \\ &- \sum_{n=2}^l \frac{2n+1}{n-1} \int_{\psi=0}^{\psi_o} P_n(\cos \psi) \sin \psi d\psi \\ &- \sum_{n=0}^l \frac{2n+1}{2} t_n(\psi_o) \int_{\psi=0}^{\psi_o} P_n(\cos \psi) \sin \psi d\psi \end{aligned} \quad (18)$$

The integral of the Stokes function can be written as (Heiskanen and Moritz 1967)

$$\int_{\psi=0}^{\psi_o} \mathcal{S}^l(\psi) \sin \psi d\psi = - \int_{\psi=\psi_o}^{\pi} \mathcal{S}^l(\psi) \sin \psi d\psi = -Q_0(\psi_o) \quad (19)$$

and the integral of Legendre's polynomial reads (Paul 1973)

$$\begin{aligned} \int_{\psi=0}^{\psi_o} P_n(\cos \psi) \sin \psi d\psi &= - \int_{\psi=\psi_o}^{\pi} P_n(\cos \psi) \sin \psi d\psi \\ &= -R_{n,0}(\psi_o) \end{aligned} \quad (20)$$

The integral on the left-hand side of Eq. (18) is then of the form (Martinec 1993)

$$\begin{aligned} \int_{\psi=0}^{\psi_o} \mathcal{S}^l(\psi, \psi_o) \sin \psi d\psi &= -Q_0^l(\psi_o) \\ &+ \sum_{n=0}^l \frac{2n+1}{2} R_{n,0}(\psi_o) t_n(\psi_o) = -\tilde{Q}_0^l(\psi_o) \end{aligned} \quad (21)$$

and the contribution of the computation point to the geoid is given by (Martinec 1993)

$$N_{\diamond}^l(\Omega) = -\frac{R\Delta g^l(\Omega)}{2\gamma} \tilde{Q}_0^l(\psi_o) \quad (22)$$

### 3.2 Contribution of the near zone from discrete numerical integration and 1D-FFT

The contribution of the remainder of the spherical cap to the high-frequency geoid can be evaluated by discrete summation over mean values of gravity anomalies on a regular geographical grid within the cap (cf. Fig. 1). After accounting for the contribution of the computation point, the contribution of the near zone to the high-frequency geoid is

$$N_{\odot-\diamond}^l(\Omega) = \frac{R}{4\pi\gamma} \iint_{\Omega_{\odot}} [\Delta g^l(\Omega') - \Delta g^l(\Omega)] \mathcal{S}^l(\psi, \psi_{\odot}) d\Omega' \quad (23)$$

Using the mean-value theorem, the integration in Eq. (23) can be replaced by the summation over  $(j-1)$  cells within the spherical cap of the product of discrete mean values of high-frequency gravity anomalies (Vaniček and Krakiwsky 1986)

$$\overline{\Delta g^l}(\Omega_k) = \frac{1}{\Delta\Omega_k} \iint_{\Omega_k} \Delta g^l(\Omega') d\Omega' \quad (24)$$

with corresponding point values of the modified spheroidal Stokes function. Equation (23) then reads

$$\begin{aligned} N_{\odot-\diamond}^l(\Omega) &= \frac{R}{4\pi\gamma} \sum_k^{j-1} \left\{ \iint_{\Omega_k} [\Delta g^l(\Omega') - \Delta g^l(\Omega)] \mathcal{S}^l(\psi, \psi_{\odot}) d\Omega'_k \right\} \\ &\doteq \frac{R}{4\pi\gamma} \sum_k^{j-1} [\overline{\Delta g^l}(\Omega_k) - \overline{\Delta g^l}(\Omega)] \mathcal{S}^l(\psi_k, \psi_{\odot}) \Delta\Omega_k \quad (25) \end{aligned}$$

where the value of  $\mathcal{S}^l(\psi_k, \psi_{\odot})$  is evaluated for the spherical distance  $\psi_k$  between the integration point and the centre of the  $k$ -th cell, and  $\Delta\Omega_k$  is the surface area of the  $k$ -th cell; see Fig. 1.

An alternative approach to the discrete numerical integration of Eq. (25) is represented by the solution in the spectral domain, which is based on the convolution theorem. Here, the discretized integration of mean gravity anomalies [Eq. (25)] may be reformulated, without further approximation, as the sum (in latitude) of a series of 1D discretized convolution integrals (in longitude). The discrete 1D-FFT, when applied to mean high-frequency gravity anomalies within the spherical cap ( $\Omega_{\odot}$ ), can be written for a fixed latitude  $\varphi_k$  of the computation point as (Haagmans et al. 1993)

$$N_{\text{FFT}}^l(\Omega) \doteq \frac{R\Delta\varphi\Delta\lambda}{4\pi\gamma} \mathcal{F}^{-1} \left\{ \sum_{k=1}^{i-1} \mathcal{F} [\overline{\Delta g}(\Omega_k) \cos \varphi_k] \cdot \mathcal{F} [\mathcal{S}^l(\psi_k, \psi_{\odot})] \right\} \quad (26)$$

where  $\mathcal{F}$  and  $\mathcal{F}^{-1}$  denote the 1D discrete Fourier transform operator and its inverse, respectively,  $i$  is the

number of gravity data along the meridian  $\varphi_k$ , and  $\Delta\varphi$  and  $\Delta\lambda$  are the sampling intervals of a regular data grid. When applied correctly to the same gravity data, both the spatial form [Eq. (25)] and spectral form [Eq. (26)] should produce an identical high-frequency geoid. Note that the spectral form also faces the problem arising from the singularity of the Stokes function and the contribution of the computation point must be evaluated separately (Haagmans et al. 1993).

Concerning the relative numerical efficiency of discrete numerical integration and 1D-FFT, it has been argued for a long time that discrete Fourier transform is computationally superior to discrete numerical integration. However, due to recent developments in discrete numerical integration (Huang et al. 2000) both methods now use a comparable amount of computational time.

### 3.3 Contribution of the distant zone from spherical harmonic coefficients

The contribution of the distant zone to the high-frequency geoid has been derived by several authors. The approach taken here, originally derived by Molodenskij et al. (1960), uses the so-called Molodenskij coefficients (weights) to account for the influence of the distant zones omitted from the truncated integration in Eq. (25) or Eq. (26). The Molodenskij coefficients for the modified spheroidal Stokes function [Eq. (10)] are (see e.g. Martinec 1993)

$$\begin{aligned} \forall m > l : \tilde{Q}_m^l(\psi_{\odot}) &= \int_{\psi=\psi_{\odot}}^{\pi} \mathcal{S}^l(\psi, \psi_{\odot}) P_m(\cos \psi) \sin \psi d\psi \\ &= Q_m(\psi_{\odot}) - \sum_{n=2}^l \frac{2n+1}{n-1} R_{n,m}(\psi_{\odot}) \\ &\quad - \sum_{n=2}^l \frac{2n+1}{2} t_n(\psi_{\odot}) R_{n,m}(\psi_{\odot}) \quad (27) \end{aligned}$$

where the spherical truncation coefficients  $Q_m(\psi_{\odot})$  are given by Eq. (14). The contribution of the distant zone to the high-frequency geoid height can then be evaluated using a conversion of the spatial form in Eq. (9) to a spectral form based on spherical harmonics (Martinec 1993)

$$\begin{aligned} N_{\oplus-\odot}^l(\Omega) &= \frac{GM}{2R\gamma} \sum_{n=l+1}^{\max} (n-1) \left(\frac{R}{r_g}\right)^{n+2} \tilde{Q}_n^l(\psi_{\odot}) T_n(\Omega) \\ &\doteq \frac{R}{2} \sum_{n=l+1}^{\max} (n-1) \tilde{Q}_n^l(\psi_{\odot}) T_n(\Omega) \quad (28) \end{aligned}$$

with the spherical harmonic coefficients of the disturbing gravity potential  $T_n$  taken from a combined global geopotential model. The maximum degree  $\max = 120$  can be used for numerical evaluations, thus rendering the effect of higher-degree terms smaller than 1 mm (Martinec 1993).

To conclude this section, the final expression for the determination of the high-frequency geoid can be written for discrete numerical integration as

$$\begin{aligned}
N^l(\Omega) &= N_{\diamond}^l(\Omega) + N_{\ominus-\diamond}^l(\Omega) + N_{\oplus-\ominus}^l(\Omega) \\
&= -\frac{R}{2\gamma} \Delta g^l(\Omega) \tilde{Q}_0^l(\psi_o) \\
&\quad + \frac{R}{4\pi\gamma} \sum_k^{j-1} \left[ \overline{\Delta g^l}(\Omega_k) - \overline{\Delta g^l}(\Omega) \right] \mathcal{S}^l(\psi_k, \psi_o) \Delta \Omega_k \\
&\quad + \frac{R}{2} \sum_{n=l+1}^{120} (n-1) \tilde{Q}_n^l(\psi_o) T_n(\Omega) \quad (29)
\end{aligned}$$

The final expression for the determination of the high-frequency geoid by 1D-FFT is then

$$\begin{aligned}
N^l(\Omega) &= N_{\text{FFT}}^l(\Omega) + N_{\oplus-\ominus}^l(\Omega) = \frac{R\Delta\varphi\Delta\lambda}{4\pi\gamma} \\
&\quad \left\{ \mathcal{F}^{-1} \left\{ \sum_{k=1}^{i-1} \mathcal{F} \left[ \overline{\Delta g}(\Omega_k) \cos \varphi_k \right] \cdot \mathcal{F} \left[ \mathcal{S}^l(\psi_k, \psi_o) \right] \right\} \right. \\
&\quad \left. + \frac{R}{2} \sum_{n=l+1}^{120} (n-1) \tilde{Q}_n^l(\psi_o) T_n(\Omega) \right\} \quad (30)
\end{aligned}$$

#### 4 Synthetic gravity field based on spherical harmonics

The test chosen to evaluate and compare the accuracy of the high-frequency geoid computation from discrete quadrature-based numerical integration [used in Eq. (29)] and discrete 1D-FFT [used in Eq. (30)] uses a self-consistent set of synthetically generated geoid heights and gravity anomalies. This approach is analogous to that taken by Tziavos (1996), who uses a degree 360 global geopotential model. However, the current study extends the upper bound of the frequencies over which the accuracy of the geoid computation can be assessed.

Over the Canadian territory, mean gravity anomalies on a regular 5' geographical grid (prepared by the Geodetic Survey Division of Natural Resources Canada) are usually used for the determination of the regional gravimetric geoid (see e.g. Sideris and She 1995; Vaníček et al. 1995). The Nyquist frequency of this gravity grid corresponds to a maximum spherical harmonic expansion of degree and order 2160. Since freely available global geopotential models only contain coefficients up to degree and order 360 [notwithstanding the GPM98 models (Wenzel 1998), which extend to degree 1800], it is necessary to artificially generate a set of synthetic coefficients complete to degree and order 2160.

The synthetic spherical harmonic expansion of the geopotential consists of two distinct parts. First, all spherical harmonic coefficients for degrees  $l+1 \leq n \leq 360$  were taken from the EGM96 global geopotential model (Lemoine et al. 1998) with respect to the GRS80 reference ellipsoid. Second, the remaining synthetic coefficients for degrees  $361 \leq n \leq 2160$  were generated from an artificially constructed sequence of pairs of real numbers. These were taken from the

EGM96 coefficient pairs of orders  $0 \leq m \leq 360$  at degree  $n = 360$ . For example, in order to generate the synthetic coefficients for degree 540, the EGM96 coefficient pairs were used for  $0 \leq m \leq 360$  and used again for  $361 \leq m \leq 540$ .

However, using only this approach yielded an unrealistic degree variance (cf. Heiskanen and Moritz 1967, p. 259) of the synthetic field, which did not agree with current expectations of the actual geopotential spectrum of the Earth (cf. Tscherning and Rapp 1974). Therefore, each pair of high-degree synthetic coefficients was multiplied by a simple scale factor to yield a more realistic degree variance (described later). The degree-360 sequence of EGM96 coefficients was thus scaled and used in a repeated cycle, until all of the required synthetic coefficients were produced. The aim of this approach was to generate a synthetic field that was reasonably realistic so that inferences made about the accuracy of the high-frequency geoid computation using the synthetic gravity field will apply to the real Earth.

The scale factor used is given by  $(a^*/a)^{n-360}$ , where  $a$  is the radius of the geocentric sphere upon which the spherical harmonic expansion of the EGM96 coefficients reduces to Laplace harmonics, and  $a^*$  is the radius of an arbitrary reference sphere that is of a similar magnitude to  $a$ , but slightly smaller. This combination of scale factor and synthetic coefficients provided a convenient means by which the degree variance of the synthetic field would smoothly extend from EGM96 into the higher degrees, while also providing a decaying degree variance similar to current expectations. Formulation of the scale factor using the  $a$  and  $a^*$  terms was effected for reasons of computational efficiency and convenience only. Therefore, no physical interpretation should be made regarding this scale factor or the synthetic gravity field.

The synthetic coefficients were used to produce two data sets with different degree variances in the high-degree terms, which was achieved by changing the  $a^*$  term. The first synthetic field, called Data A, was generated using a value of  $a^* = 6.34 \times 10^6$  m; the second synthetic field, called Data B, used  $a^* = 6.35 \times 10^6$  m. The degree variances of these two data sets were compared against the GPM98B tailored global geopotential model (Wenzel 1998) in the region  $360 \leq n \leq 1800$  in order to help ensure that the synthetic degree variances remained reasonably realistic. The value of the  $a^*$  term was selected in such a way that the high-degree frequencies of Data A were less powerful than the corresponding frequencies of GPM98B, and vice versa for Data B. The degree variances of Data A and GPM98B are shown in Fig. 2; the degree variances of Data B and GPM98B are shown in Fig. 3. Data A has less power in the very high frequencies than Data B, which is apparent from the larger amplitude of higher-frequency geoid undulations in Figs. 4 and 5.

#### 5 Methodology, results and discussion

A conceptually simple procedure, which follows that of Tziavos (1996), was employed to assess and compare the

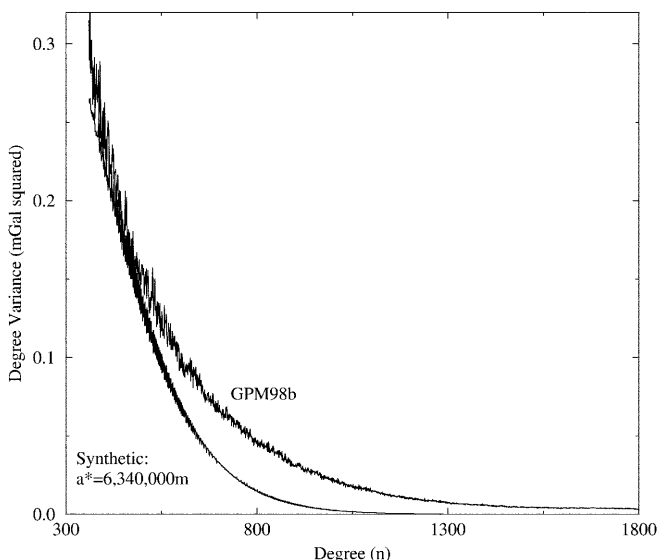


**Fig. 2.** Gravity anomaly degree variance of Data A vs GPM98B ( $\text{mGal}^2$ )

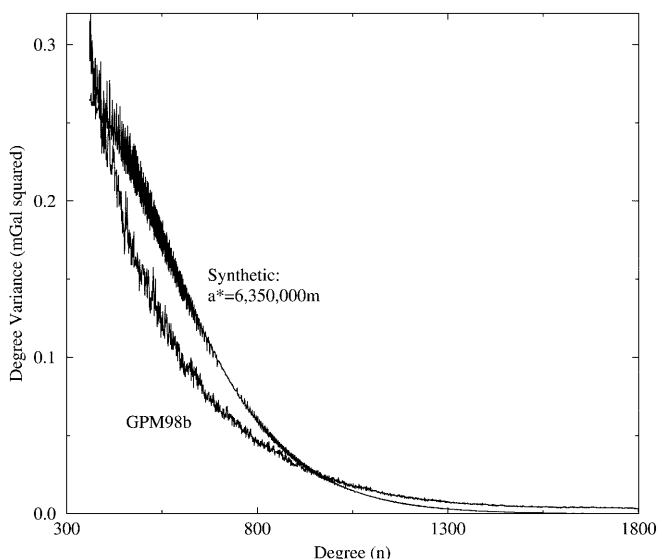


**Fig. 3.** Gravity anomaly degree variance of Data B vs GPM98B ( $\text{mGal}^2$ )

discrete numerical integration and the 1D-FFT in the modified spheroidal Stokes approach to high-frequency geoid determination. Two synthetic gravity fields were generated using the procedures described above. The synthetic gravity anomalies in the region  $21 \leq n \leq 2160$  were computed directly for each set and are designated 'Data A' and 'Data B'. The corresponding synthetic geoid heights ( $21 \leq n \leq 2160$ ) were likewise produced from each set and are designated 'Spheroid A' and 'Spheroid B'. The result is two self-consistent (to a spherical approximation) grids of geoid heights and gravity anomalies, which can be used to compare different methods for gravimetric geoid computation.

All gravity anomaly and geoid values were produced on identical, regular  $5'$  geographical grids for a test region bounded by  $49 \leq \varphi \leq 54^\circ$  (N) and  $236 \leq \lambda \leq 246^\circ$  (E). This grid spacing corresponds with the gravity anomaly grids produced by the Canadian Geodetic Survey Division. Although this area covers the Canadian Rocky Mountains, it should be remembered that the synthetic geopotential coefficients for degrees  $361 \leq n \leq 2160$  were not generated empirically from observational data. Therefore, they do not necessarily reflect the actual gravity field generated by the topography and geology of this region. Accordingly, no physical interpretation should be made from them.

The methodology is best understood by first considering the use of a single integration technique in conjunction with a single set of synthetic geoid heights and gravity anomalies. The high-frequency gravity anomalies ( $21 \leq n \leq 2160$ ) were produced by subtracting the low-degree reference spheroid of degree  $l = 20$  from synthetic gravity anomalies [Eq. (7)]. This approach was taken so as to replicate as closely as possible the approach that is used in practical geoid computations with observational gravity data. The contribution of the near zones to the high-frequency geoid ( $21 \leq n \leq 2160$ ) was then obtained from the high-frequency synthetic gravity grid using both the discrete numerical integration [in Eq. (25)] and the 1D-FFT [in Eq. (26)]. A cap radius of  $\psi_0 = 6^\circ$  was used in each technique. The contribution of the distant zones to the high-frequency geoid was, in both cases, evaluated using spherical harmonics and the coefficients from the EGM96 global geopotential model to degree max = 120 [Eq. (28)]. The computed contributions from the near and distant zones were combined to give the high-frequency residual geoid, which was added to the ( $l = 20$ ) reference spheroid to yield a total gravimetric geoid solution ( $2 \leq n \leq 2160$ ) for the test region. This process was repeated for Data A and Data B, which resulted in four gravimetric geoid solutions computed from the synthetic gravity anomalies.

Figure 6 shows a schematic of the methodology used. Theoretically, the difference between the computed and synthetic geoids should be equal to zero everywhere across each grid for both Data A and Data B. Therefore, any computed differences are used as indicators of the *accuracy* of each numerical technique (i.e. numerical integration and 1D-FFT) when used in conjunction with the high-frequency geoid determination based on the Molodenskij-modified spheroidal Stokes formula. The term *accuracy* is used here since the exact geoid heights expected from the gravity anomalies is known (to a spherical approximation) from the synthetic field.

Tables 1 and 2 show a statistical summary of the differences between each synthetic geoid and the computed geoids, as obtained using the numerical integration and 1D-FFT, respectively. These are given for Data A (the synthetic field with less power than GPM98B in the medium and high frequencies) and Data B (the synthetic field with more power than GPM98B in the medium and high frequencies). The standard deviations in Tables 1 and 2 show that both discrete numerical

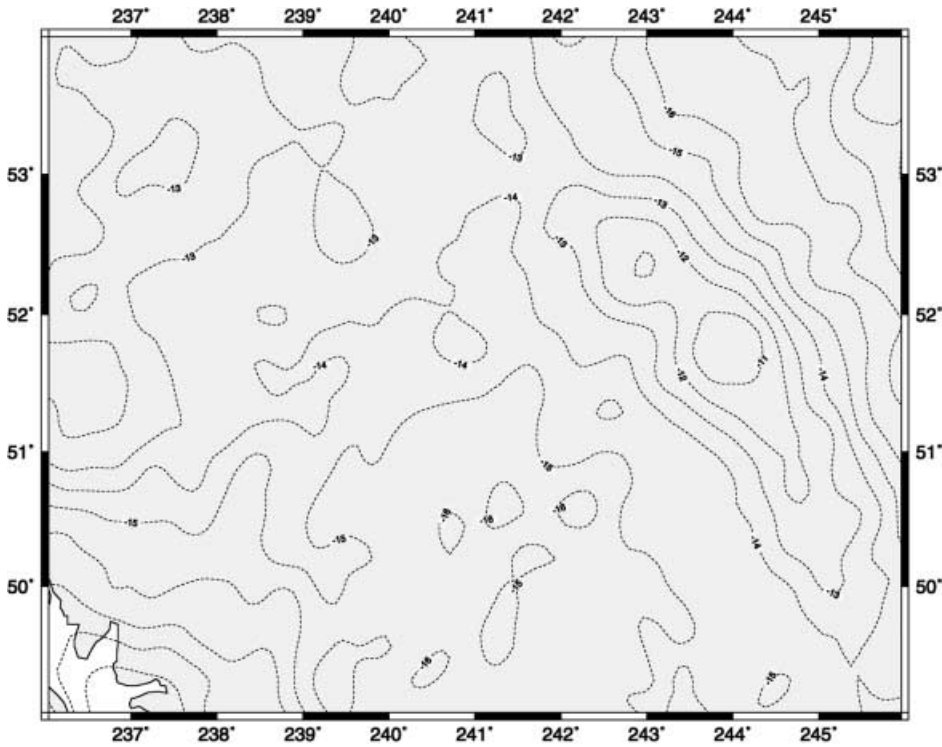


Fig. 4. Degree 2160 spheroid A (metres)

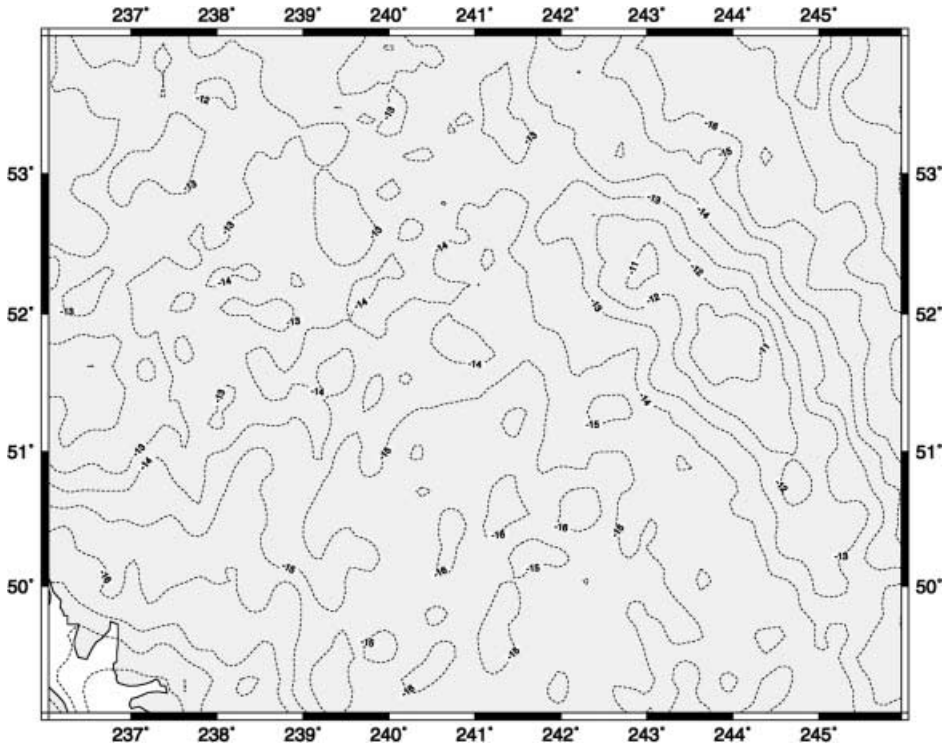


Fig. 5. Degree 2160 spheroid B (metres)

integration and 1D-FFT deliver a precision of approximately 1 cm for the test region. The range (i.e. maximum minus minimum) and standard deviation of the discrepancies obtained through the use of the numerical integration procedure are slightly smaller than those obtained from the 1D-FFT, although the im-

provement is not statistically significant and lies within the numerical accuracy of the computer algorithms used. Thus, both methods provide comparable accuracy, as one would expect from the theory. As stated earlier, the recent advances in discrete numerical integration make it as computationally fast as 1D-FFT (Huang et al. 2000).

## Scheme of the Testing Procedure

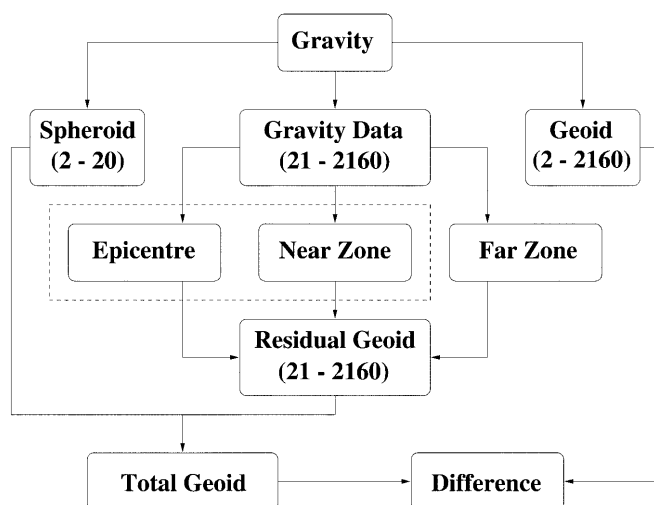


Fig. 6. Scheme of the testing procedure

**Table 1.** Statistics of the differences between the high-frequency geoid from the synthetic field and discrete numerical integration (metres)

Statistic	Data A	Data B
Maximum	+ 0.026	+ 0.039
Minimum	- 0.017	- 0.030
Arithmetic mean	+ 0.003	+ 0.003
Standard deviation	± 0.008	± 0.010

**Table 2.** Statistics of the differences between the high-frequency geoid from the synthetic field and 1D-FFT (metres)

Statistic	Data A	Data B
Maximum	+ 0.033	+ 0.045
Minimum	- 0.026	- 0.036
Arithmetic mean	+ 0.003	+ 0.003
Standard deviation	± 0.009	± 0.011

Therefore, there are no compelling arguments based on numerical accuracy or efficiency that suggest that either technique is preferable for high-frequency geoid determination; the choice of using discrete numerical integration or 1D-FFT to compute the high-frequency geoid is merely one of computational convenience.

The discrepancies observed for both numerical approaches become slightly larger for Data B than for Data A. A visual confirmation of this point may be obtained by inspection of Figs. 7 and 8, which plot the discrepancies between the synthetic geoid values and those computed using numerical integration for Data A and Data B, respectively. This result, and the results summarized in Tables 1 and 2, imply that the accuracy of each technique will decrease when applied to regions in which there is more power in the medium- and high-frequency bands of the local gravity field. From this, it

can be inferred that the accuracy of the computed geoid may be worse than 1 cm in regions of the Earth for which this is true.

In addition to comparing the numerical accuracy of discrete numerical integration and 1D-FFT, the results in Tables 1 and 2 show that the numerical implementation of the modified Stokes theory [Eqs. (29) and (30)] can yield the high-frequency ( $21 \leq n \leq 2160$ ) geoid accurate to approximately 1 cm in this test region. However, this has assumed that there are no errors in the input gravity data, which is not necessarily true when using observational gravity data.

## 6 Summary and conclusions

This contribution has reviewed the Molodenskij-modified spheroidal Stokes integral and given a strategy for its practical solution, which is based on a degree  $l = 20$  satellite-derived reference spheroid, a contribution of gravity anomalies inside a spherical cap of  $6^\circ$  radius, and a contribution from the remote zones outside this cap from a degree 120 combined global geopotential model. This has been tested against a high-frequency synthetic gravity field to quantify the accuracy of the Molodenskij-modified spheroidal Stokes approach developed at the University of New Brunswick. The numerical evaluation of the near-zone contribution to the high-frequency geoid as part of this approach has been computed using both discrete numerical integration and the 1D-FFT technique. Therefore, it has simultaneously given an accuracy evaluation of discrete numerical integration and the 1D-FFT technique.

From the comparison of the computed high-frequency geoids with the synthetic high-frequency geoid, the expected accuracy for the solution of this component of a gravimetric geoid is at the 1-cm level. It is important to state that this test really only validates the accuracy of the high-frequency component of the computed gravimetric geoid. This is because any low-frequency errors in the reference spheroid ( $n \leq 20$ ) are essentially invisible to the approach used here. Nevertheless, the tests do validate the numerical accuracy of the high-frequency geoid computations based on the Molodenskij-modified spheroidal Stokes theory. Also, the gravity and other data (such as topographical heights and densities) used in practical geoid computations do not currently allow for such a strict requirement in numerical accuracy. However, the theoretical and numerical principles are being formulated with respect to the goal of a 1-cm geoid.

In addition to verifying the appropriateness of the modified Stokes theory, this investigation has also permitted a verification of the numerical accuracy of the near-zone contribution to the high-frequency geoid, when computed from discrete numerical integration and the 1D-FFT technique. The computer algorithms for these two approaches delivered results of comparable accuracy, with the discrete numerical integration being slightly (though not significantly) more accurate. Therefore, the expected accuracy of the high-frequency

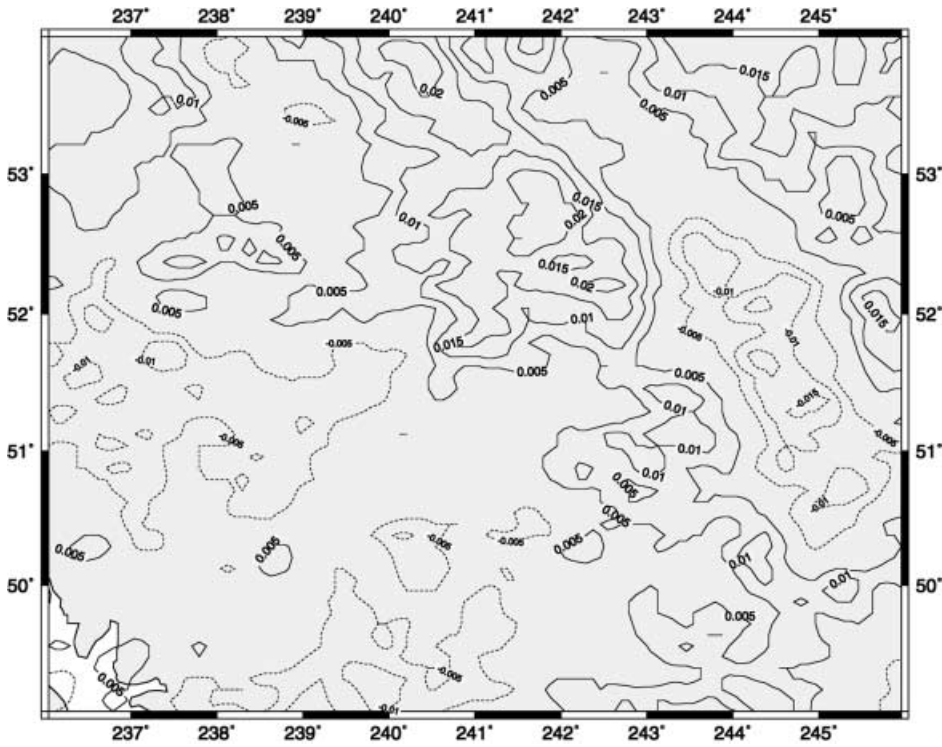


Fig. 7. Differences for the degree 2160 spheroid A (metres)

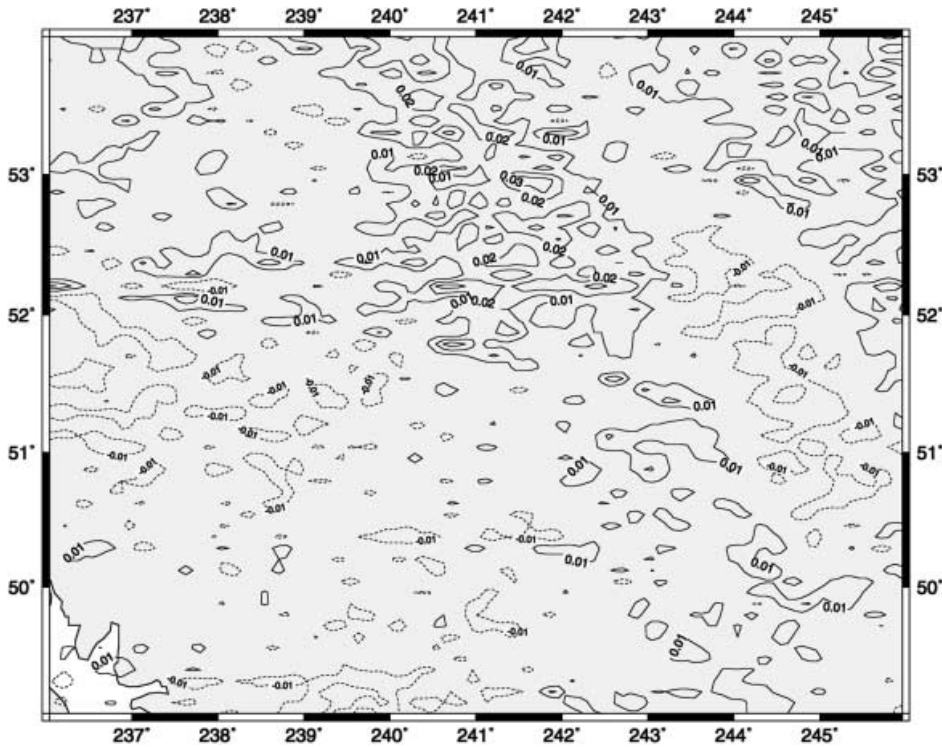


Fig. 8. Differences for the degree 2160 spheroid B (metres)

geoid computed using the Molodenskij-modified spheroidal Stokes theory (assuming error-free gravity data) is at the 1-cm level. However, it should be stressed that this value may not be achieved in practical geoid computations due to the accuracy of observational data and the approximations currently used for the regularization of the geoid.

**References**

Bruns H (1878) Die Figur der Erde. Publ des Königlichen Preussischen Geodätischen Institutes, Berlin  
 Haagsmans RRN, de Min E, van Gelderen M (1993) Fast evaluation of convolution integrals on the sphere using 1D-FFT, and a comparison with existing methods for Stokes’s integral. Manusc Geod 18: 227–241

- Heiskanen WA, Moritz H (1967) *Physical Geodesy*. Freeman, San Francisco
- Huang J, Vaniček P, Novák P (2000) An alternative algorithm to FFT for the numerical evaluation of Stokes's integral. *Stud Geophys Geod* 44: 374–380
- Lambeck K, Coleman R (1983) The Earth's shape and gravity field: a report of progress from 1958 to 1982. *Geophys J Royal Astr Soc* 74: 25–54
- Lemoine FG, Kenyon SC, Factor JK, Trimmer RG, Pavlis NK, Chinn DS, Cox CM, Klosko SM, Luthcke SB, Torrence MH, Wang YM, Williamson RG, Pavlis EC, Rapp RH, Olson TR (1998) The development of the joint NASA GSFC and NIMA geopotential model EGM96. NASA/TP-1998-206861 GSFC, Greenbelt, Maryland
- Martinec Z (1993) Effect of lateral density variations of topographical masses in view of improving geoid model accuracy over Canada. Contract report for Geodetic Survey Division, Geomatics Sector, Natural Resources Canada, Ottawa
- Martinec Z, Vaniček P (1996) Formulation of the boundary-value problem for the geoid determination with a higher-degree reference field. *Geophys J Int* 126: 219–228
- Molodenskij MS, Eremeev VF, Yurkina MI (1960) *Methods for study of the external gravitational field and figure of the Earth*. Translated from Russian by the Israel Program for Scientific Translations, Office of Technical Services, Department of Commerce, Washington, DC (1962)
- Najafi MA (1996) Contributions towards the computation of a precise regional geoid. PhD dissertation, Department of Geodesy and Geomatics Engineering, University of New Brunswick, Fredericton
- Paul M (1973) A method of evaluation the truncation error coefficients for geoidal heights. *Bull Géod* 110: 413–425
- Schwarz KP, Sideris MG, Forsberg R (1990) The use of FFT techniques in physical geodesy. *Geophys J Int* 100: 485–514
- Sideris MG, She BB (1995) A new, high-resolution geoid for Canada and part of the US by the 1D-FFT method. *Bull Géod* 69(2): 92–108
- Stokes GG (1849) On the variation of gravity on the surface of the Earth. *Trans Camb Phil Soc* 8: 672–696
- Tscherning CC, Rapp RH (1974) Closed covariance expressions for gravity anomalies, geoidal undulations, and deflections of the vertical implied by anomaly degree variance models. Rep 208, Department of Geodetic Science and Surveying, The Ohio State University, Columbus
- Tziavos IN (1996) Comparisons of spectral techniques for geoid computations over large regions. *J Geod* 70: 357–373
- Vaniček P, Kleusberg A (1987) The Canadian geoid – Stokesian approach. *Manuscr Geod* 12: 86–98
- Vaniček P, Krakiwsky EJ (1986) *Geodesy: the concepts*, 2nd corr. edn. North Holland, Amsterdam
- Vaniček P, Sjöberg LE (1991) Reformulation of Stokes's theory for higher than second-degree reference field and a modification of integration kernels. *J Geophys Res* 96: 6529–6539
- Vaniček P, Kleusberg A, Martinec Z, Sun W, Ong P, Najafi M, Vajda P, Harrie L, Tomášek P, Horst BT (1995) Compilation of a precise regional geoid. Report for the Geodetic Survey Division, Geomatics Sector, Natural Resources Canada, Ottawa
- Wenzel G (1998) Ultra-high degree geopotential models GPM98A, B, and C to degree 1800. In: Proc joint meeting of the International Gravity Commission and International Geoid Commission, 7–12 September Trieste (see also <http://www.gik.uni-karlsruhe.de/~wenzel/>)